

Computational Adsorption and Dft Studies On the Corrosion Inhibition Potentials of Some Phenyl-Urea Derivatives

*D. E. Arthur¹, A. Uzairu¹

¹Department of Chemistry, Ahmadu Bello University Zaria, Kaduna State, Nigeria.

*Corresponding author: hanslibs@myway.com

ARTICLE INFO

Article History:

Received : 10/12/2016

Accepted : 08/11/2017

Key Words:

Iron, Adsorption, Corrosion, DFT method, Fukui Function, phenyl-urea

ABSTRACT/RESUME

Abstract: The inhibition performance of [(4-Hydroxy-6-methyl-2-oxo-2H-pyran-3-yl)-phenyl-methyl]-urea and [(4-Hydroxy-6-methyl-2-oxo-2H-pyran-3-yl)-(4-methoxy-phenyl)-methyl]-urea were investigated as corrosion inhibitors using density functional theory (DFT) at the B3LYP/6-31+ G(d,p) level of theory. The calculated quantum chemical parameters correlated to the inhibition of efficiency. The molecular descriptors have been analysed through the Fukui function and local softness indices in order to compare the possible sites for nucleophilic and electrophilic attacks. The success of DFT calculation in predicting the inhibition efficiency was assessed and the result reveals that HPU2 with the adsorption energy of -91.38 kJ/mol is higher than that of HPU1 which is -394.42 kJ/mol.

I. Introduction

Corrosion of metals is probably the most pressing problem in industries today, it is a problem which has attracted the attention of so many researchers and scientist from all over the world. The protection of metal surfaces against corrosion is an important industrial and scientific topic as already noted by several authors [11]–[5].

Compounds containing heteroatoms, capable of donating lone pairs of electrons are found to be particularly useful as inhibitors for corroding metals, for instance some researchers reported the effective inhibition of corrosion of mild steel and iron by organic compounds containing heteroatoms [2], [5]–[9].

Organic compounds used as corrosion inhibitors were studied in the past, in the findings, the chemical structure and physicochemical properties of the compound like functional groups, electron density at the donor atom, p-orbital character, and the electronic structure of the molecule are primarily responsible for influencing the adsorption energy of these inhibitors onto the metal surface [6], [10]–[12].

In the present era, computer modelling techniques have been used successfully to study corrosion problems [4], [13]–[15]. Quantum chemical studies are used to analyse the inhibition efficiency of certain compounds on corrosion. One important method is the conceptual DFT which is used in calculating important reactive properties such as fukui parameters used in revealing the frontier orbitals responsible for the interaction between the metal surface and the inhibitor [16], even though conceptual DFT is basically a subfield of DFT in which one tries to extract from the electronic density. Other relevant concepts and principles that help to understand and predict the chemical behaviour of a molecule such as the hardness and softness of the species involved in this process were also used.

II. Computational Details

The present calculations were performed using Spartan 14 V 1.1.4 (Wavefunction program package) [17].

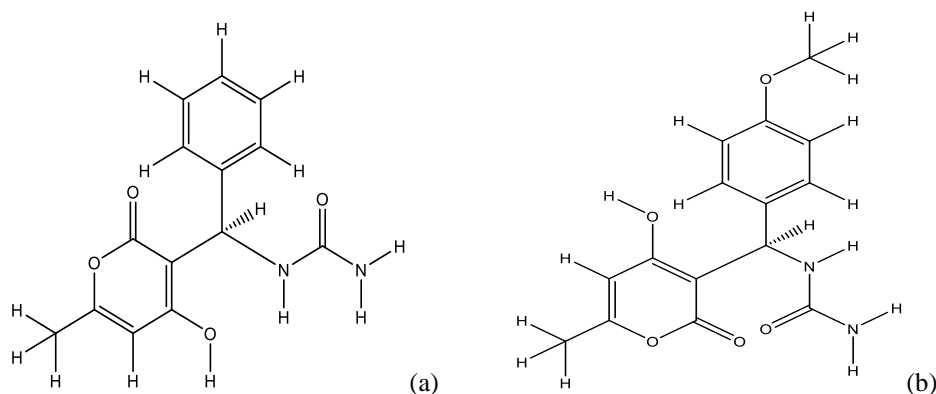


Figure 1. The molecular structures of the investigated inhibitors: (a) [(4-Hydroxy-6-methyl-2-oxo-2H-pyran-3-yl)-phenyl-methyl]-urea (HPU1) (b) [(4-Hydroxy-6-methyl-2-oxo-2H-pyran-3-yl)-(4-methoxy-phenyl)-methyl]-urea (HPU2)

Table 1. Impedance parameters for stainless steel type 316 in phosphoric acid in presence of inhibitors HPU2 and HPU1

Compound(M)	R1(Ω .cm ²)	R2(K Ω .cm ²)	C(μ F.cm ²)	IE%
Blank	3.230	1.790	63.020	-
HPU1	1.400	6.007	94.300	70.200
HPU2	1.030	8.960	159.000	80.000

The organic inhibitors used in this research work namely [(4-Hydroxy-6-methyl-2-oxo-2H-pyran-3-yl)-phenyl-methyl]-urea (HPU1) and [(4-Hydroxy-6-methyl-2-oxo-2H-pyran-3-yl)-(4-methoxy-phenyl)-methyl]-urea (HPU2) were reported by [18] to give a promising property in adopting these compounds as corrosion inhibitors since their inhibition efficiency was good, the result is explicitly shown in Table 1 and would help as a reference in justifying which of this two compounds would readily adsorb or prevent the corrosion of mild steel via adsorptive means. Where the parameters in Table 1 is defined as E% = inhibition efficiency, R1 = solution resistance, R2 = charge transfer resistance and C = double layer capacitance.

Geometry optimizations were carried out via DFT using Becke's three parameter exchange functional (B3) [19], and includes a mixture of HF with DFT exchange terms associated with the gradient corrected correlation functional of Lee, Yang, and Parr (LYP) [16] and the 6-31 + G(d,p) basis set. In the geometry optimizations process every part of the chemical structure such as its bond length and angles were freed of strain energy by first subjecting the structure to molecular mechanics (MM) calculation. The structures free from constrains were then calculated for their aqueous forms, the calculations were performed at the optimized geometries of the neutral forms (using: single point energy calculation) which prevents the odds of trying to do a geometry optimization on a species that may not be a stationary point on the potential energy surface. Frontier

molecular orbitals such as lowest unoccupied molecular orbital (LUMO) and highest occupied molecular orbital (HOMO) was used to illustrate the point of adsorption of the inhibitor molecule on the metal surface. For the simplest transfer of electrons, adsorption should occur at the part of the molecule where the softness, which is a local property, has the highest value. According to Koopman's theorem [18], the energies of the HOMO and the LUMO orbitals of the inhibitor molecule are related to the ionization potential and the electron affinity respectively (equation 1&2), by the following relationships:

$$I = -E_{Homo} \quad \text{-----} \quad (1)$$

$$A = -E_{Lomo} \quad \text{-----} \quad (2)$$

Absolute electronegativity (χ), and absolute hardness (η), of the inhibitor molecule are given in equation 3&4

$$\chi = \frac{I + A}{2} \quad \text{-----} \quad (3)$$

$$\eta = \frac{I - A}{2} \quad \text{-----} \quad (4)$$

The softness is the inverse of the hardness (equation5)

$$\sigma = \frac{1}{\eta} \quad \text{-----} \quad (5)$$

The importance of evaluating electronegativity, hardness, and softness in corrosion chemistry, have been generally accepted in effectively studying chemical reactivity involving metal interaction with

other chemical specie. The interaction of two systems such as Fe and inhibitor, suggests that electrons will drift from lower χ (inhibitor) to higher χ (Fe), until the chemical potentials come to be the same.

The amount of transported electrons (ΔN) was calculated using the equation

$$\Delta N = \frac{\chi_{fe} - \chi_{inh}}{2(\eta_{fe} + \eta_{inh})} \quad (6)$$

Where η_{fe} and η_{inh} in equation (6) represent the absolute electronegativity of iron and inhibitor molecule separately, while χ_{fe} and χ_{inh} mean the absolute hardness of iron and the inhibitor molecule, respectively.

In this study, we use the theoretical value of χ_{fe} and χ_{inh} calculated using the same level of DFT theory and basis set used to optimize the molecules, their values are reported as 0.163ev and 0.03895ev respectively for the number of transported electrons. The difference in electronegativity drives the electron transfer, and the sum of the hardness parameters acts as a resistance. The global electrophilicity index was introduced by Parr [20], [21] and is given by

$$\omega = \frac{\mu^2}{2\eta} \quad (7)$$

According to the description, this index measures the tendency of chemical species to accept electrons. A good nucleophile is characterized by lower value of χ and ω (equation 7), while for a good electrophile

a higher value of χ and ω is observed. This new reactivity index measures the balance in energy when there is an additional electronic charge ΔN from the environment to the system.

The aim of this paper is to determine the relationship between quantum chemical descriptors with the experimental inhibition efficiencies of the inhibitors by measuring the quantum chemical parameters such as the energies of highest occupied molecular orbital (EHOMO) and the lowest unoccupied molecular orbital (ELUMO), the energy difference (ΔE) between EHOMO and ELUMO, absolute electrophilicity (ω), electronegativity (χ), electron affinity (A), absolute hardness (η), softness (σ), ionization potential (I), the fraction of electrons transferred (ΔN), and the total energy (Etot) to theoretically justify the behaviours of this inhibitors with an iron surface.

III. Results and Discussion

Figure 2 shows the optimized structures of HPU1 and HPU2 inhibitors along with atomic numbering, while Figure 3 shows the LUMO and HOMO or frontier orbitals of the inhibitors.

The computed quantum chemical properties such as E_{HOMO} , E_{LUMO} , ΔE_{L-H} and dipole moment of the inhibitors (HPU1 and HPU2) optimized are reported in Table 2.

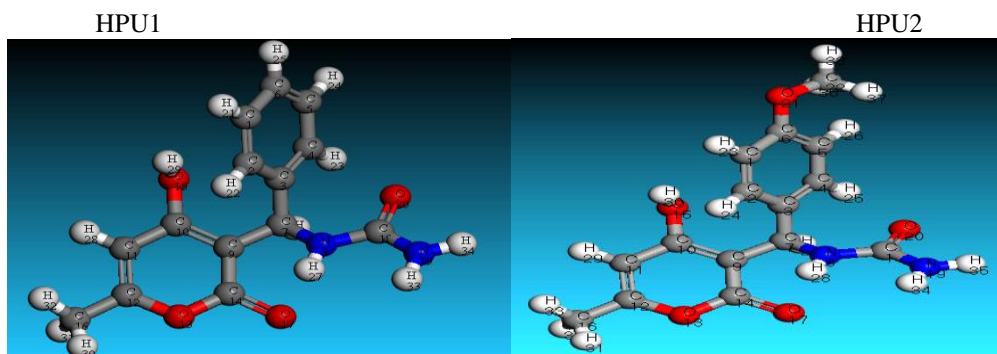


Figure 2. Optimized geometries of (a) [(4Hydroxy6methyl2oxo2Hpyran3yl) phenylmethyl] urea (HPU1) (b) [(4Hydroxy6methyl2oxo2Hpyran3yl)(4methoxyphenyl)methyl]urea(HPU2) molecules along with atomic numbering calculated at B3LYP/6-31 + G(d, p) level of theory

Table 2. Calculated quantum chemical properties for the most stable conformation of the HPU1 and HPU2 molecules calculated at B3LYP/6-31 + G(d,p) level of theory.

Quantum parameters	HPU1	HPU2
E_{Homo} (eV)	-5.96	-5.66
E_{Lumo} (eV)	-1.01	-0.96
ΔE_{L-H} (eV)	4.95	4.70
μ (debye)	1.82	1.03

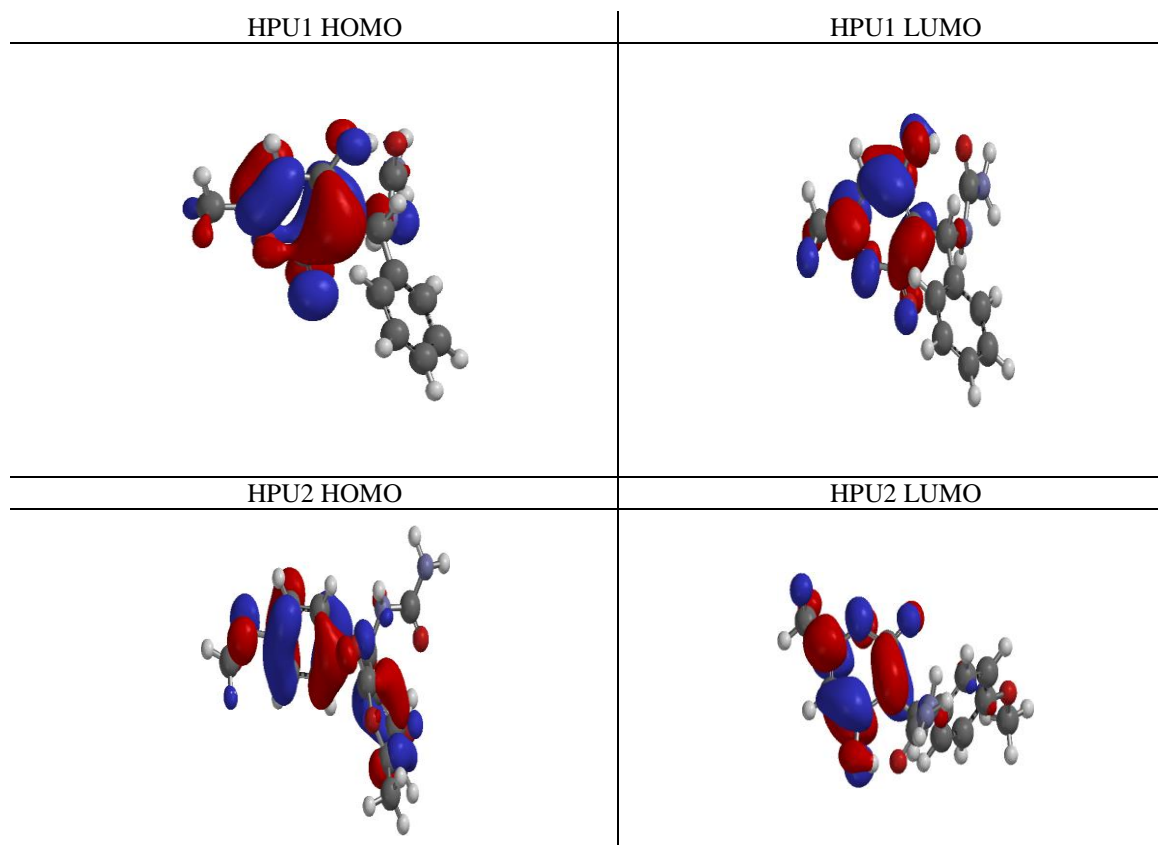


Figure 3. Frontier molecular orbitals (FMO) of HPU1 and HPU2 molecules calculated at B3LYP/6-31 + G(d,p) level of theory, the colour red represent nucleophilic parts of the compound while the blue colour represent electrophilic part.

In corrosion chemistry, inhibition of metal corrosion comes as a result of interaction between the frontier molecular orbitals of the metal surface and the inhibitor, where the cloud electrons on the metal surface is deposited on the LUMO of the inhibitor and the lone pair electrons or in anions the charged surface donates the bonding electron into the d-orbital of the metal [22], [23]. The LUMO energy of HPU2 (-0.96 eV) is less negative than that of HPU1 which is -1.01 and because of the excess electron on the metal surface the HPU2 inhibitor, the LUMO of HPU2 will readily accept some of the excess electron from the surface of the metal thereby making HPU2 molecule more liable for interaction.

The energy gap is another parameter necessary in explaining DFT studied reactions, it serves as a function of reactivity of the inhibitor molecule towards the adsorption on the metal surface [24]. Energy gap defines the stability of a chemical specie in a chemical environment, its decrease can be related to the increase in the reactivity of the molecule towards to better inhibition efficiency [16]. HPU2 inhibitor has the lowest energy gap (4.70 eV) when compared to HPU1 inhibitor (4.95 eV) which can be seen in Table 2, the difference in their energy gap is approximately equal to 0.25 eV which is enough to

make a difference in this system [25]; this means that HPU2 molecule could have better performance as corrosion inhibitor than HPU1 molecule, a deduction that totally agrees with the experimental finding [18].

The dipole moment (μ) for HPU1 and HPU2 were also calculated, it is an electronic parameter that describes the extent of charge distribution around the surface of the molecule, it can be used to predict the reactivity and stability of molecules [26]. The high value of dipole moment leads to an increase in deformation energy, making the adsorbed molecule at the ferrous surface rather unstable and unsuitable as a corrosion inhibitor [1], [27], [28].

In Table 2, the dipole moment of HPU2 (1.03 Debye) supports the experimental result, which claims HPU2 is a better inhibitor when compared to 1.82 Debye of HPU1 [29]. Other computed quantum chemical properties such as ionization energy, electron affinity, absolute electronegativity, absolute hardness, absolute softness, absolute electrophilicity, the fraction of electron transferred, and the total energy for HPU1 and HPU2 inhibitors are reported in Table

Table 3. Calculated quantum chemical parameters of HPU1 and HPU2 molecules calculated at B3LYP/6-31 + G (d,p) level of theory in atomic units

Quantum parameters	HPU1(au)	HPU2 (au)
$I = -E_{\text{Homo}}$	0.219	0.208
$A = -E_{\text{Lumo}}$	0.037	0.035
$\chi = \frac{I + A}{2}$	0.128	0.122
$\eta = \frac{I - A}{2}$	0.091	0.086
$\sigma = \frac{1}{\eta}$	11.008 au⁻¹	11.607 au⁻¹
$\omega = \frac{\mu^2}{2\eta}$	43.883	13.350
$\Delta N = \frac{\chi_{\text{fe}} - \chi_{\text{inh}}}{2(\eta_{\text{fe}} + \eta_{\text{inh}})}$	20.174	18.553
E_{tot}	-952.351	-1066.873

Ionization energy (I) and electronegativity (χ) are important molecular descriptors to be considered when studying chemical reactions involving inorganic species like metals and molecules, they were calculated for HPU1 and HPU2 and reported in Table 3. High ionization energy indicates high stability and chemical inertness while high electronegativity is the opposite [30]. The high ionization energy of HPU2 (0.208 au) and Low electronegativity (0.035 au) supports its high inhibition efficiency than when compared to HPU1 whose ionization energy and electronegativity given as 0.219 au and 0.037 au respectively clearly indicates that HPU2 will readily react with the metal surface than HPU1.

Absolute hardness (η) and softness (σ) of HPU1 and HPU2 were also calculated and reported in Table 3 reflects on the measure of molecular stability and reactivity of the inhibitors. A hard molecule has a large energy gap and a soft molecule has a small energy gap [24]. In this study HPU2 with low hardness value $\eta = 0.086$ au. compared to that of the HPU1 $\eta = 0.091$ au. The absolute softness was found to be higher in HPU2 (11.607 au) than HPU1 (11.008 au) which supports the experimental result since the inhibition efficiency is higher in HPU2 than in HPU1 [18].

The number of electrons transferred (ΔN) was also calculated and tabulated in Table 3. If $\Delta N < 3.6$, the inhibition efficiency increases and in return increasing the electron-donating ability of these metals to donate electron to the metal

surface [10] and the results indicate that ΔN values for the inhibitors HPU1 and HPU2 supports the experimental inhibition efficiencies.

The total energy of HPU2 inhibitor is $E_{\text{tot}} = -1066.873$ au, while for HPU1 inhibitor it is $E_{\text{tot}} = -952.351$, this tends to support the argument on which inhibitor active centres would favour adsorption process on the metal surface. From the result stated in Table 3, HPU2 would adsorb more and prevent corrosion of the mild steel more than HPU1, this agrees well with the experimental inhibition efficiency reported by [1].

IV. Computational Adsorption Study

The calculations were performed by means of the DFT electronic structure programme DMol3 using a Mulliken population analysis, frequency, Fukui function and orbital analysis [31]. Electronic parameters for the simulation include restricted spin polarization using the DND basis set and the Perdew–Wang (PW) local correlation density functional. Geometry optimization was achieved using COMPASS II force field and the Smart minimize method by high-convergence criteria. This was followed by modelling the molecular electronic structures, including the distribution of frontier molecular orbitals and Fukui indices to establish the active sites as well as the local reactivity of the molecules.

Non-covalent adsorption of the different molecules on the Fe surface was analysed at a molecular level by molecular dynamics (MD) simulations. This was achieved using Forcite quench molecular dynamics in the Material Studio Modelling 7.0 software to sample many different low energy configurations and identify the low energy minima [13], [32]. Calculations were carried out in a 12 X 8 supercell using the COMPASS force field and the Smart algorithm. The Fe crystal was cleaved along the (110) plane. Temperature was fixed at 350 K, with NVE (microcanonical) ensemble, with a time step of 1 fs and simulation time 5 ps. The system was quenched every 250 steps.

Figure 4 shows the energy of HOMO and LUMO of the optimized adsorption structures for single molecules of HPU1 and HPU2 on the Fe (110) surface. From our simulations, the molecules can be seen to orient on the Fe surface using the frontier orbitals as shown in Figure 4B, the simulation as expected shows the Atom (O₂₀) pointing directly towards the surface of the metal, this was supported by the result of the Fukui indices for electrophilic attack in which the atom has the highest value i.e ($f^- = 0.208$).

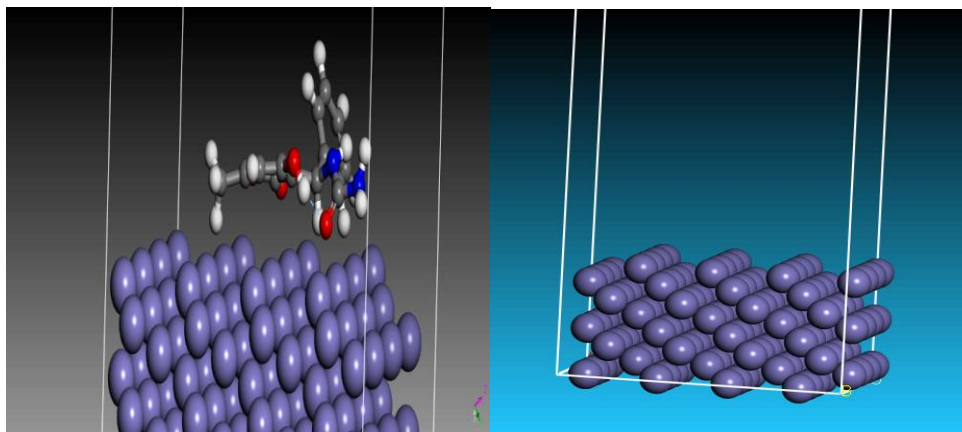


Figure 4. A diagram of Fe surface and adsorption of HPUI on the Fe surface shown in B

The Adsorption isotherm task in adsorption calculates adsorption isotherms for an adsorbent or a mixture of adsorbates in an adsorbent framework from a series of fixed pressure simulations at different pressures. During the course of the simulation, adsorbate molecules within the framework are randomly rotated and translated, and, in addition, adsorbates are randomly created in and

deleted from the framework. The configuration that results from one of these steps is accepted or rejected according to the selection rules of the Monte Carlo method being used for the simulation. The total energy of the sorption process as well as the adsorption energy and deformation energy were calculated and reported for HPU1 and HPU2 in Table 4 and 6 respectively.

Table 4: Calculated adsorption Parameters for HPUI adsorbent on the Fe (110) surface.

Total energy (kJ/mol)	Adsorption energy (kJ/mol)	Rigid adsorption energy (kJ/mol)	Deformation energy (kJ/mol)
-259.37	-394.42	-87.31	-307.11

Table 5. Fukui indices for nucleophilic and electrophilic attacks in HPUI calculated at LDA/PWC hybrid functional and DND basis set level of theory

Fukui Indices for Electrophilic Attack (Fukui (f-))			Fukui Indices for Nucleophilic Attack (Fukui (f+))		
atom	Mulliken	Hirshfeld	atom	Mulliken	Hirshfeld
C (1)	0.045	0.054	C (1)	0.010	0.009
C (2)	0.026	0.033	C (2)	-0.017	-0.001
C (3)	0.011	0.049	C (3)	-0.008	-0.004
C (4)	0.026	0.050	C (4)	0.008	0.008
C (5)	0.038	0.041	C (5)	0.009	0.011
C (6)	0.057	0.071	C (6)	0.009	0.011
C (7)	-0.010	0.006	C (7)	-0.005	0.009
N (8)	0.025	0.033	N (8)	-0.013	0.000
C (9)	0.001	0.001	C (9)	0.057	0.068
C (10)	0.005	0.007	C (10)	0.108	0.108
C (11)	0.010	0.010	C (11)	0.057	0.067
C (12)	0.010	0.012	C (12)	0.104	0.106
O (13)	0.009	0.010	O (13)	0.080	0.088
C (14)	0.012	0.008	C (14)	0.086	0.083
O (15)	0.014	0.023	O (15)	0.050	0.053
C (16)	0.000	0.004	C (16)	-0.004	0.029
O (17)	0.012	0.014	O (17)	0.122	0.114
C (18)	0.067	0.055	C (18)	0.011	0.009

N (19)	0.044	0.060	N (19)	0.007	0.009
O (20)	0.208	0.208	O (20)	0.014	0.014
H (21)	0.039	0.026	H (21)	0.009	0.006
H (22)	0.038	0.021	H (22)	0.012	0.005
H (23)	0.050	0.027	H (23)	0.010	0.006
H (24)	0.036	0.023	H (24)	0.009	0.006
H (25)	0.042	0.029	H (25)	0.008	0.006
H (26)	0.034	0.016	H (26)	0.034	0.019
H (27)	0.032	0.021	H (27)	0.014	0.009
H (28)	0.010	0.006	H (28)	0.057	0.036
H (29)	0.019	0.012	H (29)	0.033	0.029
H (30)	0.005	0.003	H (30)	0.037	0.024
H (31)	0.006	0.004	H (31)	0.047	0.034
H (32)	0.005	0.003	H (32)	0.034	0.023
H (33)	0.040	0.032	H (33)	0.005	0.004
H (34)	0.036	0.029	H (34)	0.006	0.005

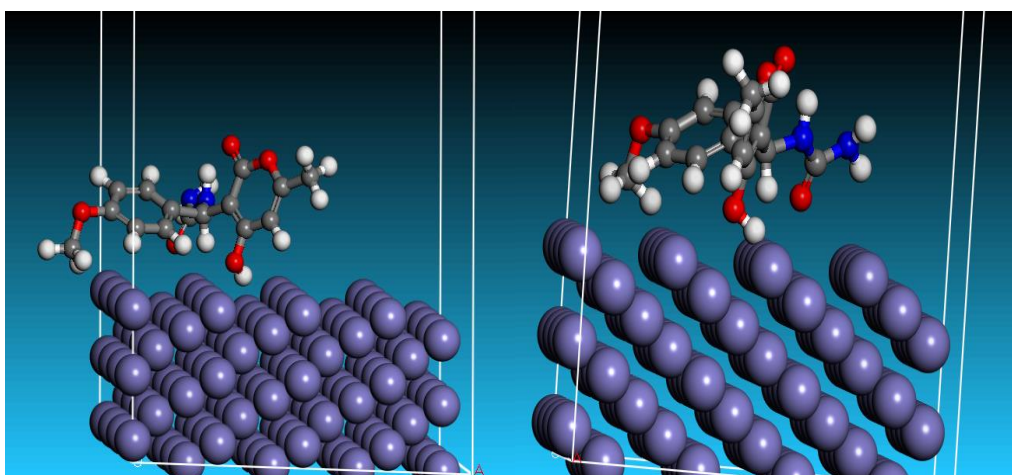


Figure 5. A sorption diagram of HPU2 adsorbate on the Fe surface shown from different side view of the cleaved (110) plane.

Table 6. Calculated adsorption Parameters for HPU2 adsorbent on the Fe (110) surface

Total energy (kJ/mol)	Adsorption energy (kJ/mol)	Rigid adsorption energy (kJ/mol)	Deformation energy (kJ/mol)
-269.62	-91.38	-99.43	8.05

The result of the adsorption parameters calculated from the sorption study of HPU1 and HPU2 on the cleaved Fe (110) surface shown in Figure 5 and reported in Table 4 and Table 6 respectively for the adsorbates shows that the total energy required for the adsorption of HPU2 (-269.62kJ/mol) is lower than that of HPU1 (-259.37), which indicates that the adsorption of HPU2 on the Fe (110) cleaved surface

is more likely than that of HPU1. The rigid adsorption energy and deformation energy of HPU2 further supports the stability of the adsorbate on Fe surface over HPU1, further emphasis could be laid on the result of the Fukui indices for both compounds presented on Table 5 and 7, this result computationally explains why HPU2 inhibits corrosion much more than HPU1.

Table 7. Fukui indices for nucleophilic and electrophilic attacks in HPU2 calculated at LDA/PWC hybrid functional and DND basis set level of theory.

Fukui Indices for Electrophilic Attack (Fukui (f-))			Fukui Indices for Nucleophilic Attack (Fukui (f+))		
atom	Mulliken	Hirshfeld	atom	Mulliken	Hirshfeld
C (1)	0.054	0.053	C (1)	0.011	0.009
C (2)	0.030	0.042	C (2)	-0.017	-0.002
C (3)	0.032	0.064	C (3)	-0.003	-0.003
C (4)	0.047	0.051	C (4)	0.008	0.008
C (5)	0.053	0.058	C (5)	0.008	0.009
C (6)	0.053	0.068	C (6)	0.007	0.008
C (7)	-0.006	0.008	C (7)	-0.008	0.008
N (8)	0.030	0.046	N (8)	-0.015	-0.001
C (9)	0.004	0.002	C (9)	0.060	0.069
C (10)	0.006	0.009	C (10)	0.107	0.108
C (11)	0.013	0.012	C (11)	0.056	0.067
C (12)	0.012	0.014	C (12)	0.105	0.107
O (13)	0.011	0.014	O (13)	0.079	0.088
C (14)	0.021	0.013	C (14)	0.085	0.082
O (15)	0.016	0.026	O (15)	0.048	0.052
C (16)	0.000	0.004	C (16)	-0.004	0.029
O (17)	0.032	0.036	O (17)	0.122	0.114
C (18)	0.028	0.028	C (18)	0.011	0.009
N (19)	0.038	0.042	N (19)	0.008	0.009
O (20)	0.063	0.062	O (20)	0.016	0.015
O (21)	0.075	0.075	O (21)	0.005	0.005
C (22)	-0.018	0.016	C (22)	-0.002	0.002
H (23)	0.043	0.028	H (23)	0.009	0.005
H (24)	0.042	0.023	H (24)	0.010	0.004
H (25)	0.044	0.026	H (25)	0.009	0.005
H (26)	0.041	0.026	H (26)	0.007	0.004
H (27)	0.033	0.015	H (27)	0.034	0.019
H (28)	0.033	0.021	H (28)	0.015	0.009
H (29)	0.011	0.007	H (29)	0.057	0.035
H (30)	0.021	0.013	H (30)	0.033	0.030
H (31)	0.006	0.004	H (31)	0.037	0.024
H (32)	0.007	0.005	H (32)	0.047	0.033
H (33)	0.006	0.004	H (33)	0.034	0.023
H (34)	0.021	0.018	H (34)	0.005	0.004
H (35)	0.022	0.019	H (35)	0.007	0.005
H (36)	0.026	0.016	H (36)	0.002	0.001
H (37)	0.029	0.017	H (37)	0.003	0.002
H (38)	0.023	0.014	H (38)	0.003	0.002

V. Conclusions

From the result of the DFT corrosion study and simulated annealed sorption study, HPU2 molecule is found to possess molecular indices or descriptors that explains and supports the experimental result of inhibition efficiency been higher than that of HPU1[18]. The adsorption energy of HPU2 is reported be -91.38kJ/mol and that of HPU1 is given as -394.42 kJ/mol, both adsorption energies supports a chemisorption process but favours the adsorption of HPU2 more.

VI. Bibliographic References

1. P.Udhayakala, T. V Rajendiran, and S. Gunasekaran, "Theoretical Evaluation of Corrosion Inhibition Performance of Some Triazole Derivatives," *Adv. Sci. Res.*, vol. 3, no. 2, pp. 71–77, 2012.
2. E. E. Ebenso, M. M. Kabanda, T. Arslan, M. Saracoglu, and F. Kandemirli, "Quantum Chemical Investigations on Quinoline Derivatives as Effective Corrosion Inhibitors for Mild Steel in Acidic Medium," *Molecules*, vol. 7, pp. 5643 – 5676, 2012.
3. N. O. Eddy, U. J. Ibok, E. E. Ebenso, A. El Nemr, E. Sayed, and H. El Ashry, "Quantum chemical study of the inhibition of the corrosion of mild steel in H₂SO₄ by some antibiotics," pp. 1085–1092, 2009.
4. N. O. Eddy, "Experimental and theoretical studies on

- some amino acids and their potential activity as inhibitors for the corrosion of mild steel , part 2 q.” *J. Adv. Res.*, vol. 2, no. 1, pp. 35–47, 2011.
5. P. O. Ameh and N. O. Eddy, “Characterization of Acacia Sieberiana (AS) Gum and Their Corrosion Inhibition Potentials for Zinc in Sulphuric Acid Medium,” vol. 1, no. 1, pp. 25–36, 2014.
 6. S. A. Umoren, “Polymers as Corrosion Inhibitors for Metals in Different Media - A Review,” pp. 175–188, 2009.
 7. M. A. Amin, S. S. A. Ei-rehim, E. E. F. El-sherbini, O. A. Hazzazi, and M. N. Abbas, “Polyacrylic acid as a corrosion inhibitor for aluminium in weakly alkaline solutions . Part I: Weight loss , polarization , impedance EFM and EDX studies,” *Corros. Sci.*, vol. 51, no. 3, pp. 658–667, 2009.
 8. V. M. Abbasov, H. M. A. El-lateef, L. I. Aliyeva, E. E. Qasimov, I. T. Ismayilov, and A. H. Tantawy, “Applicability of Novel Anionic Surfactant as a Corrosion Inhibitor of Mild Steel and for Removing Thin Petroleum Films from Water Surface,” vol. 1, no. 2, pp. 18–23, 2013.
 9. D. E. Arthur, C. E. Gimba, and E. O. Nnabuk, “Miscibility Studies of Cashew Gum and Khaya Gum Exudates in Dilute Solution by Viscometry and FTIR Analysis .,” no. 8, pp. 1–12, 2014.
 10. N. A. Wazzan and F. M. Mahgoub, “DFT Calculations for Corrosion Inhibition of Ferrous Alloys by Pyrazolopyrimidine Derivatives,” vol. 2014, no. February, pp. 6–14, 2014.
 11. M. M. Antonijevic and M. B. Petrovic, “Copper Corrosion Inhibitors . A review,” vol. 3, pp. 1–28, 2008.
 12. D. E. Arthur, A. Jonathan, P. O. Ameh, and C. Anya, “A review on the assessment of polymeric materials used as corrosion inhibitor of metals and alloys,” pp. 1–9, 2013.
 13. N. Boussalah, S. Ghalem, S. El Kadiri, B. Hammouti, and R. Touzani, “Theoretical study of the corrosion inhibition of some bipyrazolic derivatives: a conceptual DFT investigation.”
 14. Z. El Adnani, A. T. Benjelloun, M. Benzakour, M. Mcharfi, M. Sfaira, T. Saffaj, and M. E. Touhami, “DFT-based QSAR Study of Substituted Pyridine-Pyrazole Derivatives as Corrosion Inhibitors in Molar Hydrochloric Acid,” vol. 9, pp. 4732–4746, 2014.
 15. M. Ghiasi, S. Kamalinalahad, M. Arabieh, and M. Zahedi, “Carbonic anhydrase inhibitors : A quantum mechanical study of interaction between some antiepileptic drugs with active center of carbonic anhydrase enzyme,” *Comput. Theor. Chem.*, vol. 992, pp. 59–69, 2012.
 16. W. Yang and R. G. Parr, “Hardness, softness, and the Fukui function in the electronic theory of metals and catalysis.,” *Proc. Natl. Acad. Sci. U. S. A.*, vol. 82, no. October, pp. 6723–6726, 1985
 17. K. M. Manamela, L. C. Murulana, M. M. Kabanda, and E. E. Ebenso, “Adsorptive and DFT Studies of Some Imidazolium Based Ionic Liquids as Corrosion Inhibitors for Zinc in Acidic Medium,” vol. 9, pp. 3029–3046, 2014.
 18. K. Hnini, S. Fadel, M. Abderrahim, E. L. Mhammedi, and A. Chtaini, “The Inhibition Effect of Heterocyclic Compounds towards the Corrosion of Iron in Phosphoric Media,” pp. 1–13, 2015.
 19. C. Lee, W. Yang, and R. G. Parr, “Development of the Colle-Salvetti correlation-energy formula into a functional of the electron density,” *Phys. Rev. B*, vol. 37, no. 2, pp. 785–789, 1988.
 20. A. Ponti, “DFT-BASED CHEMICAL REACTIVITY INDICES.”
 21. M. Torrent-Sucarrat, F. De Proft, P. W. Ayers, and P. Geerlings, “On the applicability of local softness and hardness.,” *Phys. Chem. Chem. Phys.*, vol. 12, no. October 2009, pp. 1072–1080, 2010.
 22. T. Joseph, H. Tresa, C. Y. Panicker, K. Viswanathan, M. Dolezal, and C. Van Alsenoy, “Spectroscopic (FT-IR , FT-Raman), first order hyperpolarizability , NBO analysis , HOMO and LUMO analysis of N - [(4- (trifluoromethyl) phenyl) pyrazine- 2-carboxamide by density functional methods,” *Arab. J. Chem.*, 2013.
 23. M. G. Elghalban, A. M. El Defarwy, R. K. Shah, and M. A. Morsi, “ α -Furil Dioxime : DFT Exploration and its Experimental Application to the Determination of Palladium by Square Wave Voltammetry,” vol. 9, pp. 2379–2396, 2014.
 24. L. H. Mendoza-Huizar and C. H. Rios-Reyes, “Chemical reactivity of Atrazine employing the Fukui function,” *J. Mex. Chem. Soc.*, vol. 55, no. 3, pp. 142–147, 2011.
 25. S. Leitch, A. Moewes, L. Ouyang, W. Y. Ching, and T. Sekine, “Properties of non-equivalent sites and bandgap of spinel-phase silicon nitride,” *J. Phys. Condens. Matter*, vol. 16, no. 36, p. 6469, 2004.
 26. J. A. Seetula, R. June, and A. October, “Kinetics of the R + Cl (R = CH Cl , CHBrCl , CCl and CH CCl) reactions . An ab initio study of the transition states,” pp. 3561–3567, 1998.
 27. [H. E. Gottlieb, V. Kotlyar, and A. Nudelman, “NMR chemical shifts of common laboratory solvents as trace impurities,” *J. Org. Chem.*, vol. 62, no. 21, pp. 7512–7515, 1997.
 28. S. Riahi, S. Eynollahi, S. Soleimani, M. R. Ganjali, P. Norouzi, and H. M. Shiri, “Application of DFT method for determination of IR frequencies and electrochemical properties of 1,4-dihydroxy- 9,10-anthraquinone-2-sulphonate,” *Int. J. Electrochem. Sci.*, vol. 4, pp. 1407–1418, 2009.
 29. N. O. Obi-Egbedi, I. B. Obot, M. I. El-Khaiiry, S. A. Umoren, and E. E. Ebenso, “Computational simulation and statistical analysis on the relationship between corrosion inhibition efficiency and molecular structure of some phenanthroline derivatives on mild steel surface,” *Int. J. Electrochem. Sci.*, vol. 6, pp. 5649–5675, 2011.
 30. A. K. Chandra and M. T. Nguyen, “Use of local softness for the interpretation of reaction mechanisms,” *Int. J. Mol. Sci.*, vol. 3, pp. 310–323, 2002.
 31. E. E. Oguzie, S. G. Wang, Y. Li, F. H. Wang, E. E. Oguzie, S. G. Wang, Y. Li, and F. H. Wang, “Influence of Iron Microstructure on Corrosion Inhibitor Performance in Acidic Media Influence of Iron Microstructure on Corrosion Inhibitor Performance in Acidic Media,” 2009.
 32. E. E. Oguzie, C. E. Ogukwe, J. N. Ogbulie, F. C. Nwanebu, C. B. Adindu, I. O. Udeze, K. L. Oguzie, and F. C. Eze, “Broad spectrum corrosion inhibition: corrosion and microbial (SRB) growth inhibiting effects of,” vol. 47, no. 8, pp. 3592–3601, 2012.

Please cite this Article as:

Arthur D.E., Uzairu A., Computational Adsorption and Dft Studies On the Corrosion Inhibition Potentials of Some Phenyl-Urea Derivatives, *Algerian J. Env. Sc. Technology*, **3:3-B (2017) 559-568**